Design of a fast in situ infrared diagnostic tool

Design of a fast *in situ* infrared diagnostic tool

M. F. A. M. van Hest, A. Klaver, D. C. Schram, and M. C. M. van de Sanden[a)]
Eindhoven University of Technology, P.O. Box 513, 5600 MB Eindhoven, The Netherlands

(Received 15 July 2002; accepted 3 January 2003)

Conventional Fourier transform infrared (FTIR) spectroscopes cannot be used to perform real time *in situ* infrared reflection absorption spectroscopy at monolayer sensitivity for high deposition rates (a couple of tens to hundreds of nm/s) which can be obtained when using an expanding thermal deposition plasma. Therefore a new analysis tool has been developed. The tool is based on a fast optical scanner in combination with conventional grating technology. This results in a loss of spectral range with respect to FTIR spectroscopes, but a significant gain is obtained in time resolution. For the combination used this makes it possible to measure at time resolution as low as 1.3 ms and resolution of 24 cm^{-1} at 1000 cm^{-1}. The absorption sensitivity for single reflection at the best time resolution is approximately 10^{-2}, but can be improved by using signal enhancement techniques. Here attenuated total reflection is used and the best sensitivity obtained is approximately 10^{-3}, which is close to monolayer sensitivity for various absorption bands in the infrared spectrum of silicon oxide films. Monolayer sensitivity can be obtained by averaging multiple spectra, however this will cause the time resolution to decrease. © *2003 American Institute of Physics.*
[DOI: 10.1063/1.1564273]

I. INTRODUCTION

A commonly used method for the analysis of thin film materials is Fourier transform infrared (FTIR) reflection absorption spectroscopy (see, e.g., Refs. 1–3). This technique can be used *in situ* and in order to obtain monolayer sensitivity the absorption signal needs to be enhanced. Enhancement of the absorption signal can be obtained by implementing an attenuated total reflection (ATR) crystal (see, e.g., Refs. 4 and 5). Due to this crystal the infrared light reflected will have multiple interactions with the deposited thin film, instead of just one in single reflection mode. The absorption signal enhancement can be up to a factor of 100 and is dependent on the dimensions of the ATR crystal and the angle of reflection within the crystal. With this technique it is possible to measure the absorption of very thin films down to less than one monolayer, depending on the type and strength of absorption. The absorption signal can also be enhanced by using a metal substrate or an optical cavity substrate.[6–8] However, optical cavity substrates only enhance the absorption over limited wavelength which depends on the substrate chosen. For every wavelength interval another substrate is needed and therefore these kinds of substrates are less easy to use than an ATR crystal. With the use of metal substrates enhancement of the signal is smaller than with optical cavity substrates or ATR crystals, which makes these kinds of substrates less suitable for obtaining enhancement large enough to obtain monolayer sensitivity.

Due to the usually low deposition rates of various thin film materials (up to 1 nm/s) *in situ* FTIR reflection absorption spectroscopy has enough time resolution. With fast sampling (rapid scanning) an interval of 500–7500 cm^{-1} can be measured and with reasonable signal to noise ratio in about 0.1 s. With the improvement of deposition methods and the resulting higher deposition rates conventional FTIR reflection absorption spectroscopy as a real time *in situ* diagnostic is pushed to its limits. At the deposition rates obtained using an expanding thermal plasma (ETP) deposition method, like that used, e.g., at the Eindhoven University of Technology,[9–13] this conventional FTIR reflection absorption spectroscopy analysis method can no longer be used as an *in situ* tool if one wants to study film growth *in situ* with monolayer sensitivity. Simple calculation shows that the deposition of one single monolayer takes less than 10 ms at a deposition rate of 30 nm/s and less than 1 ms at a deposition rate of 300 nm/s. These are rates that can be obtained with the ETP deposition method.

To improve the time resolution during infrared reflection absorption experiments it was necessary to develop a new and faster *in situ* diagnostic tool. The minimum specifications for this new setup together with specifications of the conventional FTIR setup are given in Table I where it can be seen that only two parameters have to be improved and in the others there is some degree of freedom. The new setup is a compromise between offering some of the strong properties of FTIR spectroscopy and gaining time resolution. The heart of the new setup was found to be a grating which is mounted on a high speed optical scanner. So a high speed monochromator was constructed. The largest negative effect of introducing the grating will be on the spectral range of the fast infrared reflection absorption setup with respect to the conventional FTIR reflection absorption spectroscope as will be explained in this article.

In the remainder of this article the new setup will be described in depth. A detailed description of the individual components of the setup will be given, as well as the motivation for why these specific components were chosen.

[a)]Electronic mail: m.c.m.v.d.sanden@tue.nl

TABLE I. Overview of minimum specifications and FTIR equivalents.

Parameter	Minimum	FTIR (typical)
Spectral range	Dependent on absorption[a]	500–7500 cm^{-1}
Time resolution	1.0–2.0 ms	0.1–1.0 s
Resolution	25 cm^{-1}	8–16 cm^{-1}
Sensitivity	2×10^{-4} (monolayer, Si–O–Si)	10^{-2} with averaging

[a]For the setup used in this article a spectral range of 700–1400 cm^{-1} was used.

Based on specifications of the different components an estimate of the expected signal to noise ratio will be given. This is followed by experimental results that demonstrate that the new method is operational and conform its design specifications. The use of the fast infrared reflection absorption spectroscope will be illustrated by the fast deposition of silicon oxide-like films of hexamethyldisiloxane (HMDSO) and oxygen on silicon substrates and ZnSe ATR crystals.

II. FAST INFRARED SPECTROSCOPE

A schematic overview of the optics of the fast infrared reflection spectroscope is shown in Fig. 1. The light emitted by a cascaded arc light source (1) is converted into a parallel beam (2) and is guided through a reflection absorption spectroscopy setup (3)–(9) after which the exiting parallel beam is reflected onto the surface of a grating (10) and focused (11) onto an infrared detector (13). Just before reaching the detector the light beam passes through a filter (12), which suppresses second and higher order diffraction of the grating.

A. Light source

A cascaded arc is used as a light source (1), because it has a higher infrared light intensity than the more commonly used globars in FTIR spectroscopes.[14–16] A detailed description of the light source was given by Wilbers *et al.*[15,16] and by Raghavan *et al.*[14] The light source used is operated with argon at pressure of 1.8 bar and argon flow of 10 sccm. The operating current was set to 25 A and the light that exited the window of the arc is KBr with a thickness of 4 mm. Measurements of the light beam emitted by the arc show that the divergence of the beam exiting the arc is 75 mrad and that the radiating surface is 3×10^{-4} m^2. Light output of the light source, in the spectral range used in the rest of this article, is mainly influenced by the arc operating current and the gas pressure. (It is known that changing the gas from argon to xenon has a positive influence on the light intensity.[15]) Increasing the arc current has a strong influence on the light intensity, an increase of 10% in the current results in an increase of 10% in the light intensity emitted. A 10% increase of gas pressure however results in only a 5% increase of emitted light intensity. Limitations imposed by the window thickness (pressure) and the power supply (current) resulted in the operating conditions used.

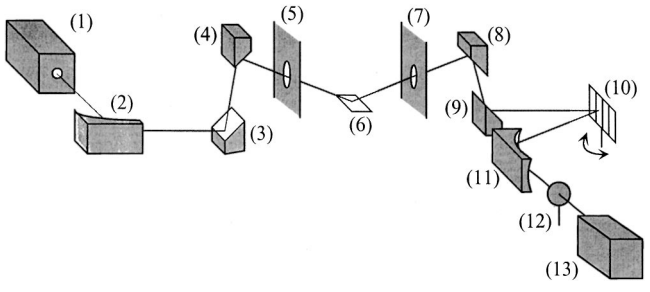

FIG. 1. Schematic overview of the fast infrared reflection absorption setup: (1) light source, (2) 90° off axis parabolic mirror ($f=19$ cm), (3) flat gold coated mirror, (4), 90° off axis parabolic mirror ($f=36$ cm), (5) KBr window in vessel wall, (6) substrate, (7) KBr window in vessel wall, (8) 90° off axis parabolic mirror ($f=36$ cm), (9) flat gold coated mirror, (10) grating on an optical scanner, (11) 90° off axis parabolic mirror ($f=7.5$ cm), (12) filter, and (13) detector.

B. Grating on the optical scanner

In conventional FTIR spectroscopy a broadband spectrum (typical spectral range of 500–7500 cm^{-1}) is measured by a scanning mirror interferometer, which is the heart of a FTIR spectroscope. Due to movement of one of the two mirrors in the interferometer Fourier transform of the light spectrum is generated. By measuring the light intensity as a function of the mirror position and by Fourier transforming the resulting interferogram a broadband light intensity spectrum is obtained. The resolution of this kind of spectroscope is dependent on the displacement of the scanning mirror.[5,17] Larger displacement results in higher resolution. The speed of the interferometer is the main reason the time resolution is not high. In short, it is fair to say that in a FTIR spectroscope the interferometer works as a medium that identifies separate wavelengths.

In the fast infrared reflection absorption spectroscopy setup a dispersive medium is used to separate light into its individual components. As a result, only a limited wavelength interval will be detected by the detector at any one time, whereas in FTIR spectroscopy all the light is detected by the detector at the same time.[5,17] This results in a lower absolute detector signal intensity in the new situation compared to FTIR spectroscopy, due to which noise induced by a background signal will become relatively more important in the new situation.

A grating is used as a dispersive medium. To calculate dispersion a grating equation is used,[18,19]

$$a(\sin\theta_i+\sin\theta_m)=m\lambda, \tag{1}$$

where a is the spacing of the groove, m the order of diffraction, λ the wavelength, and θ_i and θ_m the angle of incidence and the angle of diffraction, respectively. By rotating the grating and keeping the detector at a fixed position, both the incident and diffraction angles change simultaneously, which is identical to the procedure used in most monochromators.[19–21]

As stated before the use of the fast infrared absorption reflection spectroscope will be shown by means of the fast deposition of silicon oxide-like films. Therefore the grating was chosen such that it is possible to measure in the wavelength interval from 700 to 1400 cm^{-1}. In this interval there is absorption of both the Si–O and Si–CH_x bonds present which have an absorption width of several tens of wave numbers. Using the grating equation [Eq. (1)] with normal incidence (0.0 rad) and a refraction angle of approximately

0.5 rad at 1050 cm^{-1} (center of the interval), it can be calculated that it is best to use a grating of 53 grooves/mm. This exact grating is not commercially available and therefore a blazed grating of 50 grooves/mm was used. Changing the setup for other wavelengths can be done by changing the grating, filter, and/or detector.

The grating is positioned on top of an optical scanner (Cambridge Technology Inc. model 6650) which is capable of oscillating the grating at frequency of up to 300 Hz (sinusoidal) with angle large enough to pass the desired wavelength interval along the detector. This wavelength interval is smaller than the interval that can be measured with the FTIR spectroscope, because of the limited rotational angle of the optical scanner at such high oscillation frequencies. Therefore it is not possible to monitor film absorption at positions in the absorption spectrum which are not within the range scanned by the grating at the same time. Notice that the maximum rotational angle is dependent on the mass of the grating and the frequency. Increasing the oscillating frequency or the grating mass results in a decrease in maximum rotational angle.

Because the grating oscillates on top of the optical scanner it is possible to measure the spectrum for both forward and backward motion of the oscillation. Therefore the acquisition speed of the spectra will be twice the oscillation frequency. So at an oscillating frequency of 300 Hz the spectra are obtained at 600 Hz, and the measuring time scale is equal to 1.3 ms, which is equal to the time scale needed for monitoring monolayer film growth at a growth rate of approximately 230 nm/s. To monitor even higher film growth rates another optical scanner would be needed. The reproducibility of the angle of the optical scanner is within 6 μrad. This is accurate enough to be negligible with respect to the measuring interval of the detector signal and the scanner position signal. Note that in the grating equation the change in incident and diffracted angles is the same as the rotational angle of the scanner. Furthermore, the maximum rotational angle of the scanner is twice the oscillation amplitude.

C. Mirrors

The setup consists of a total of six mirrors. For the mirrors that focus [(4) and (11)] and defocus [(2) and (8)] a light beam 90° off axis parabolic mirror was used. This was done to reduce aberrations obtained using spherical mirrors. The disadvantage of using 90° off axis parabolic mirrors is that they are less easy to align than spherical mirrors due to their strict 90° positioning.[22]

In order not to lose too much intensity due to reflection of the mirrors, four of the six mirrors were covered with a thin gold coating. The other two [(4) and (5)] are not coated. This is because these two 90° off axis parabolic mirrors had to be custommade because they have a focal length (36 cm) which is not commercially available.

D. Windows

The infrared reflection absorption spectroscope is used to monitor *in situ* the film deposition and therefore two windows have to be mounted in the deposition reactor wall. KBr was chosen as the window material, just as it was for the light source, because it has good transparency in the wavelength range of interest. A disadvantage of using KBr windows is that they are hygroscopic, and therefore less useful when wants to measure a water absorption signal.

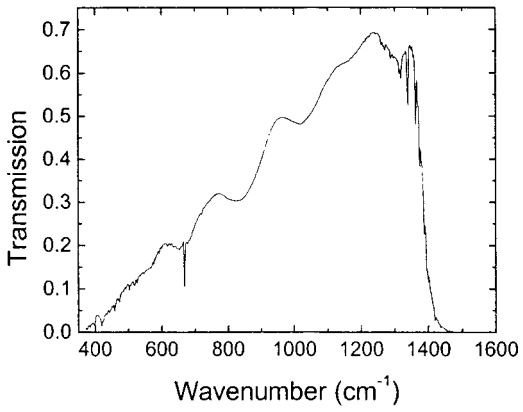

FIG. 2. Transmission profile of the cutoff filter.

E. Filter

The main part of the fast reflection absorption spectroscope is the grating. A disadvantage of using the grating is that instead of only getting first order diffraction second and higher order diffraction also appears. These higher orders interfere with first order and therefore have to be filtered. The interfering wavelength (λ_{int}) can be given by

$$\lambda_{int}=\frac{\lambda_1}{m}, \quad m\geqslant 2, \tag{2}$$

where λ_1 is the first order wavelength and m the order of the interfering light. Light interfering with first order light is always smaller in wavelength. Therefore to remove higher orders a filter is needed that transmits the desired wavelength and absorbs the lower wavelengths. The cutoff needs to be somewhere between the lowest wavelength desired and half the highest wavelength desired. A transmission profile of the filter used is given in Fig. 2. As can be seen the filter used does transmit light in the desired range (700–1400 cm^{-1}) up to 70% of its original intensity. The cutoff at 1400 cm^{-1} is in agreement with the desired wavelength band. The filter has to be changed when the grating is changed for measurements in another wavelength interval.

F. Detector

To detect the infrared light a mercury–cadmium–telluride (MCT) detector (type D316) was used. Due to its high sensitivity to infrared light MCT detectors have a fairly high dark current induced by background radiation (see, e.g., Ref. 23). For this reason generally MCT detectors are equipped with a double amplifier, i.e., a dc amplifier followed by an ac amplifier, with fixed amplification factors. However, for the new infrared reflection absorption spectroscope it is better to only dc amplify the detector signal. This is in order to have a direct correlation between the detector signal and the infrared light intensity of the detector. By

installing a variable resistor on the amplifier it is possible to subtract the dark current signal from the detector signal and by installing a second variable resistor also the amplification factor of the amplifier was changed to maximize the detector output voltage. The detector response time, including the amplifier, is equal to 5 μs.

G. Data acquisition and control

The signal of the detector as well as the signal that indicates the position of the optical scanner are measured by a 16-bit 200 ksamples/s analog to digital converter (ADC) card (National Instruments 6035E) inside a PC. The measurements are controlled by the same computer using dedicated software which was programmed into National Instruments CVI LABWINDOWS. In the software code a part was integrated which can be used to analyze the measured data.

The number of data points measured to record one single spectra (N) is given by

$$N=\frac{1}{2f_{\mathrm{osc}}}\frac{f_{\mathrm{sample}}}{N_{\mathrm{channels}}}, \tag{3}$$

where f_{osc} is the optical scanner oscillation frequency and f_{sample} is the ADC sampling rate. N_{channels} is equal to the number of channels used for measuring, which is fixed to two, one for the detector and one for the optical scanner position. In the case where the setup is used at 300 Hz and the ADC sampling frequency is set to its maximum value, the number of data points for one single spectrum will equal 167. Roughly speaking, approximately every 4 cm^{-1} a data point is obtained, which is enough to have several data points within one single solid state absorption band (typical width 10–50 cm^{-1}). When the setup is operated at a lower oscillating frequency the number of data points per spectra will increase and the spectral measuring interval will decrease. At the maximum ADC sampling frequency the detector signal is measured every 10 μs which is twice the response time of the detector.

The detector position signal is also measured every 10 μs. The total rotational angle of the scanner is 0.1 rad and therefore the position is measured every 0.6 mrad when the scanner is scanning at a constant velocity. This 0.6 mrad is much larger than the 6 μrad positioning accuracy of the optical scanner, and therefore errors due to positioning of the scanner can be neglected.

III. THEORY

A. Spectral resolution

When the detector area is infinitesimally small, the light source would be a point source and the optics would be aligned perfectly, and the wavelength interval detected at any one time would be unique for every measuring time. However, due to the dimensions of the detecting area of the detector a small wavelength interval will be detected. The grating is responsible for the dispersion of light and therefore the grating determines the wavelength interval of the detector. In Fig. 3 a schematic of the grating, focusing mirror, and detector is given ($L_1=20$ cm). In Fig. 3 the final focusing mirror

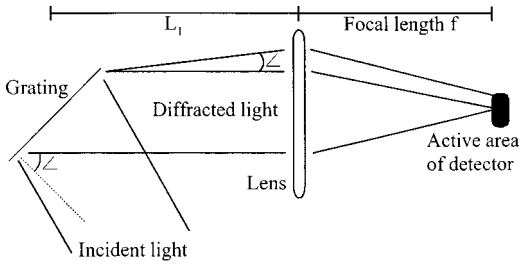

FIG. 3. Schematic of the path of light from the grating to the detector.

(cf. Fig. 1) is presented as a lens. From this plot it can be seen that indeed a small wavelength interval is focused onto the active detector area. Although the focusing mirror is presented as a lens, this has no consequences for the shown effect. Using the grating equation [Eq. (1)] and lens theory, it follows that the wavelength interval of the detector, and thus the resolution, is about 24 cm^{-1} at 1000 cm^{-1}. In lens theory, the angle of θ is determined by the focal length (f) and the size of the detector area (a). $\theta=\tan^{-1}(0.5*a/f)$. This width is less than the separation of the absorption peak of various absorption peaks of the silicon oxide-like film absorption spectrum in the range of 700–1400 cm^{-1}. Therefore the individual absorption bands in the silicon oxide-like film absorption spectrum can be identified in the reflection absorption spectrum. Also, the resolution calculated is better than the minimum value given in Table I.

B. Signal intensity

To be able to estimate the number of photons that will be collected by the detector, and the resulting detector signal, the number of photons emitted by the light source as well as the geometrical and optical losses need to be known. In the following this estimate will be made, in a worst case approach, from light source to detector.

C. Source intensity

Raghavan *et al.*[14] showed that the cascaded arc light source in the infrared can be modeled as a blackbody radiator with temperature (T) of 12 000 K and emissivity of 20%. The number of photons emitted per second per solid angle of blackbody radiator as a function of the wavelength [$N(\lambda)\times(\mathrm{s}^{-1}\,\mathrm{sr}^{-1})$] is given by the Planck blackbody radiation equation:

$$N(\lambda)=\frac{c}{\lambda^4}\frac{1}{\exp(hc/\lambda kT)-1}, \tag{4}$$

with c the speed of light, h the Planck constant, and k the Boltzmann factor. It has been shown that always a small wavelength interval (24 cm^{-1}) is on the detector. So by integrating Eq. (4) over this wavelength interval the number of photons emitted by the light source can be calculated. Including the opening angle, the emitting surface area, and the emissivity efficiency it is found that the light source emits a minimum of 2.0×10^{17} photons/s in any one wavelength interval detected by the detector in the desired spectral range. Not all photons emitted by the light source will reach the detector. Photons will be lost because of two reasons. First,

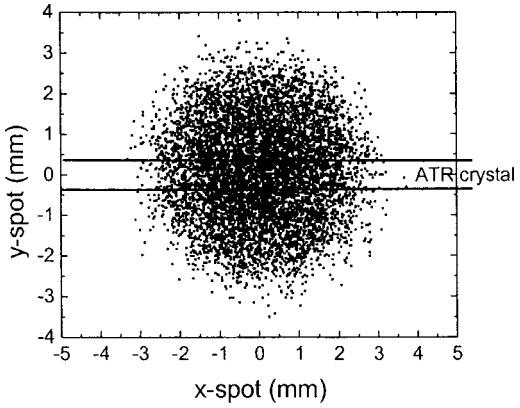

FIG. 4. Spot on the initial beveled surface of the ATR crystal obtained from ray trace simulations.

by means of geometrical loss of various optical elements and, second, by optical loss during reflection and transmission at and through the various optical elements.

D. Geometrical losses

To calculate the geometrical losses of the setup a ray trace simulation of the setup was performed. For this calculation the setup was slightly simplified. First, all 90° off axis parabolic mirrors were modeled as ideal infinitesimal thin lenses. This will have no effect on the final result as long as the opening angle is the same. Second, all flat mirrors were left out of the simulation, which is allowed because due to their size no light will fall outside the mirror surface and thus there is no geometrical loss. The total geometrical loss of the setup is dependent on the kind of sample used. In case the setup is used in single reflection mode, the sample will be large in comparison to the spot size on the sample and therefore there will be no geometrical loss at the sample. In contrast when the setup is used in ATR mode the spot size on the initial beveled surface of the ATR crystal will be larger than this surface and therefore significant loss will result at the beveled surface. In Fig. 4 the light spot on the initial beveled surface of the ATR crystal is shown. It can be seen clearly that a large amount of light is lost at this initial beveled surface. The spot size is approximately 6 mm in diameter and the ATR crystal has a width of 20 mm and a height 0.7 mm. Therefore approximately 80% of the light on the initial surface of the ATR crystal does not enter the crystal and is lost. The spot size of 6 mm at the initial beveled surface of the ATR crystal is due to an inaccurate focal length of the 90° off axis parabolic mirror that focuses light onto the initial beveled surface. The focal length is 36 cm whereas a focal length of 45 cm would have been better, but as mentioned earlier these 90° off axis parabolic mirrors had to be custommade and 36 cm was the largest focal length that could be manufactured.

From the simulation it can be concluded that when the setup is used in single reflection mode, the total geometrical transmission is equal to 70%. The main geometric losses are on the first KBr window (15%) and on the detector (10%). When using the setup in ATR mode, the geometrical setup transmission drops to a mere 15%.

TABLE II. Reflection and transmission coefficients for various elements of the setup.

Element	Transmission/reflection coefficient
Gold coated mirror	98% reflection
Aluminum mirror	70% reflection
KBr window	80% reflection
Grating	70% reflection
Filter	70% transmission
Substrate	70% reflection
ZnSe ATR crystal	70% transmission

E. Optical losses

The different elements in the setup will all have nonperfect transmission or reflection, due to which part of the light will be lost upon interaction of the light with the various elements. This loss can be calculated by means of simple calculation. In Table II the reflection and transmission coefficients of the various elements in the setup are given. For the grating not only the reflection coefficient is important, the efficiency also has to be known. The efficiency is equal to the fraction of total incident light which will be reflected into first order. This efficiency is at least 30%.[24]

By considering all the elements in the setup, the total optical losses can be calculated. They are found to be equal to 96.8% and practically independent of the setup's operating mode. This is because the ZnSe ATR crystal transmission loss is approximately equal to the silicon substrate reflection loss. The main loss is on the grating and on the custommade aluminum 90° off axis parabolic mirrors.

F. Detector

Considering the amount of photons emitted by the light source and the geometrical and optical losses of the setup elements, it is found that about 5×10^{15} photons per second per detected wavelength interval (24 cm^{-1}) will arrive on the detector surface when the system is used in single reflection mode. In the spectral range for which the setup was initially designed the detector used has a minimum detection efficiency of 60%, and the energy flux detected by the detector will be at least 7.3×10^{-5} W. Depending on detector amplifier settings this energy flux will result in a lower limit for the maximum detector signal of 2.2 V. The noise in the detector signal is approximately 20 mV and therefore a theoretical signal to noise ratio of 10^2 can be obtained. With this signal to noise ratio it is possible to measure absorption intensities of 1% and higher when the system is used in single reflection mode and no spectra are averaged. In the case where the setup is used in ATR mode without anything else changed, the detector signal measured will go down by approximately one order of magnitude, but nevertheless the minimum detectable absorption intensity will increase.

Note that in calculation of the light intensity a worst case scenario was used therefore the maximum signal measured is higher than this calculated value. The intensity calculation was done in the wavelength interval having the lowest light intensity and the lowest detector sensitivity was used. However, in the range used the detector has the highest sensitivity

TABLE III. Summary of various parameters for the fast infrared reflection absorption spectroscopy setup.

Parameter	Fast grating spectroscope
Spectral range	700–1400 cm^{-1}
Time resolution	$\geqslant$1.3 ms
Resolution	24 cm^{-1}
Sensitivity at best time resolution	1×10^{-2} single reflection 1×10^{-3} ATR crystal

in the wavelength interval in which the light intensity emitted by the light source is the lowest. Therefore the maximum signal measured by the detector will be higher than its calculated value and thus the best signal to noise ratio will be higher than its calculated value. A rough estimate shows that this value will be 50%–100% higher.

Aside from the photons emitted by the light source which end up on the detector surface photons emitted by various elements in the direct vicinity of the detector will also end up on the detector surface, causing the signal measured to increase with an offset. A significant part of this offset can be subtracted from the measured signal electronically, but still the value will be dependent on the angle of the grating because the number of background photons collected by the detector will be different for different grating positions. Later in this article how to eliminate the total background signal will be shown.

A summary of the various parameters of the fast infrared reflection absorption spectroscopy setup is given in Table III. As can be seen time resolution of 1.3 ms is obtained for which still a signal to noise ratio of 10^2 is obtained in single reflection. Nevertheless, to do this spectral range and resolution had to be offered with respect to FTIR reflection absorption spectroscopy.

IV. REFLECTION ABSORPTION SPECTRA

To obtain a reflection absorption spectrum with the fast infrared reflection absorption spectroscope a couple of steps have to be taken. First, a background spectrum and a reference spectrum have to be obtained; they are shown in Fig. 5. The background spectrum is the spectrum as a function of the optical scanner angle obtained when the light source is turned off. It can be seen in Fig. 5 that the detector intensity is not constant as a function of the optical scanner position. This is due to the infrared light emitted by various objects in close vicinity to the infrared reflection absorption spectroscopy setup.

Absorption is measured relative to a reference. The reference is obtained by measuring the light intensity as a function of the optical scanner angle when the light source is turned on. For the reference spectrum shown in Fig. 5 a bare silicon sample was used as a reflector. Notice that the reference spectrum closely resembles the filter profile (cf. Fig. 2), from which it can be concluded that the light source is continuous with nearly constant intensity in the range of measurement.

It can also be seen in Fig. 5 that the reference spectrum consists of two parts. A sudden increase in intensity is observed at 0.0 rad after which the remaining part of the measured spectrum resembles the first part of the spectrum. The intensity however is less than that of the first part of the spectrum. This is not a real change in intensity for wavelengths corresponding to the angle indicated, but it is second order diffraction of the grating for the wavelengths which are transmitted by the filter. Because it is second order diffraction, according to the grating equation [Eq. (1)], it needs to have double the width of the other part of the spectrum. Therefore the part seen is second order of the part of the spectrum observed between -0.175 and -0.125 rad and not of the whole spectrum observed between -0.175 and 0 rad. The reason for not observing the whole second order spectrum of the light transmitted is because of the blaze angle of the grating. This causes the intensity of the light diffracted at angles larger than 0.100 rad to decrease rapidly.

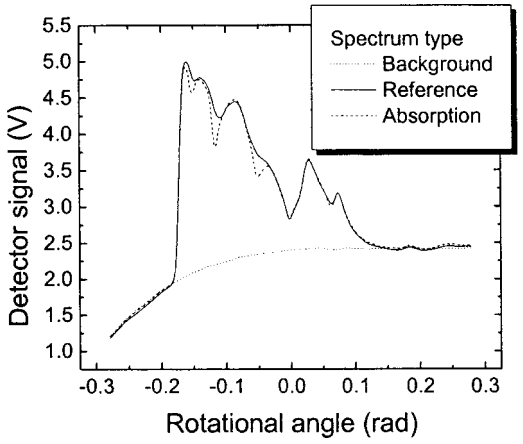

FIG. 5. Raw signal from the infrared reflection absorption spectroscope.

To calculate the reflection absorption spectrum a measured intensity spectrum $[I(\varphi)]$, in which part of the intensity is absorbed, is also needed. The reflection absorption spectrum $[R(\varphi)]$ can be calculated by

$$R(\varphi)=\frac{I(\varphi)-I_{\text{back}}(\varphi)}{I_0(\varphi)-I_{\text{back}}(\varphi)}, \tag{5}$$

where $I_0(\varphi)$ is the reference spectrum obtained without absorption and $I_{\text{back}}(\varphi)$ is the background spectrum obtained when the light source was turned off. In Fig. 5 an absorption spectrum is shown that was obtained by introducing an absorber in the reflecting light beam. By means of Eq. (5) the absorption spectrum as a function of the optical scanner position of the measured intensity data is calculated and the result of this calculation is shown in the image on the left in Fig. 6.

V. WAVELENGTH CALIBRATION

In general it is rather difficult to measure the angle of incidence and the angle of diffraction at the grating accurately enough to use the grating equation to calculate the wavelength as a function of the optical scanner position. Therefore a wavelength calibration has to be performed. The easiest way to perform a wavelength calibration is by means of gas phase absorption: first, because in general the spectral position of gas phase absorption is known well and, second, because gas phase absorption bands have small widths com-

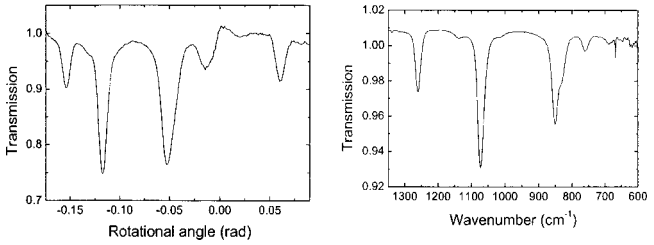

FIG. 6. HMDSO gas phase absorption measured with the fast infrared reflection absorption spectroscope (left) and with the FTIR gas phase absorption spectroscope (right).

pared to solid state absorption bands. So, in addition to gas phase absorption measurements, some information about the profile of the apparatus (resolution) of the fast infrared reflection absorption spectroscopy setup is also obtained. To calibrate the setup in the range of 700–1400 cm^{-1} HMDSO gas was used. In the range given this molecule has four absorption bands, shown in Table IV.

With the aligned fast infrared reflection absorption spectroscopy setup gas phase absorption can be measured. A blank silicon substrate is used as a reflector, the pump line is closed, and 50 Pa HMDSO is let into the reactor. In both the incident light beam to the sample as the reflected infrared beam from the sample gas phase absorption will take place. By measuring the infrared spectrum with and without the HMDSO gas present it is possible to calculate the absorption spectrum as a function of the optical scanner position.

In Fig. 6 an absorption spectrum measured by the fast infrared reflection absorption spectroscope is shown. This spectrum was calculated using the measurements in Fig. 5. Notice that there is no difference between calculating a reflection absorption spectrum and a gas phase absorption spectrum. The absorption spectrum shown was calculated by using Eq. (5).

In Fig. 6 the absorption spectrum obtained by the more conventional FTIR gas phase absorption spectroscopy technique is also shown. A comparison of the two absorption spectra immediately shows that there are five absorption peaks in the fast infrared reflection absorption spectrum and there are only four absorption peaks in the FTIR gas phase absorption spectrum. This difference is due to the fact that the absorption peaks in the fast infrared reflection absorption setup can also be seen in their second order diffraction from the grating. So the first absorption peak (shown on the left) has the same origin as the last absorption peak (shown on the right). When the absorption intensity of these two absorption peaks is compared it can be seen that the absorption intensity is the same.

TABLE IV. Overview of different gas absorption bands of HMDSO in the range of 700–1400 cm^{-1} (after Refs. 30 and 31).

Bond	Type of vibration	Wave number (cm^{-1})
$Si–CH_3$	Symmetrical bending	1260
Si–O–Si	Asymmetrical stretching	1070
$Si–CH_3$	Asymmetrical rocking	850
$Si–CH_3$	Asymmetrical bending	758

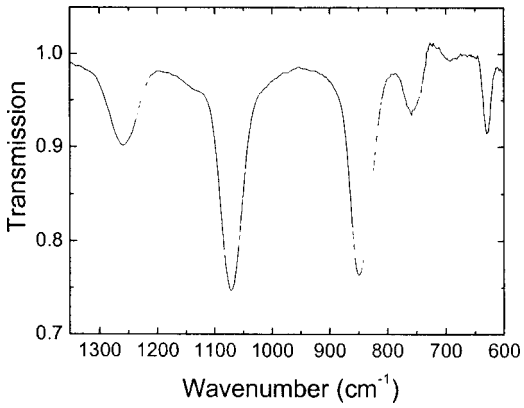

FIG. 7. Spectrum of HMDSO gas phase absorption with the converted optical scanner position.

Note that there is a difference between the absorption intensity measured with the fast infrared reflection absorption setup and that with the FTIR gas phase absorption setup. This is mainly due to a difference in the gas pressure used, but it is also due to a difference in resolution. A comparison of the noise level of both methods using the spectra shown in Fig. 6 is not valid because for the FTIR spectroscopy measurements 100 spectra were averaged and for the fast infrared reflection spectroscope no spectra were averaged. Also, the path length between the two methods is different because the FTIR spectroscopy measurement is a straight through measurement (5 cm above and parallel to the substrate) and for the fast infrared reflection spectroscope the infrared light beam passes through the reactor at some angle and is reflected at the surface, causing the path length to be longer.

By using absorption peak positions conversion of the optical scanner angle position to wave numbers can be made using Eq. (1). For the absorption spectrum shown in Fig. 6 this was done and the result of this conversion is shown in Fig. 7. Comparison of this absorption spectrum with the spectrum measured by FTIR gas phase absorption spectroscopy shows that in FTIR spectroscopy the resolution is independent of the position in the spectrum whereas that is not the case for the fast infrared reflection absorption spectroscope. Due to the use of a grating the resolution in wavelength measured is close to constant, but due to the fact that conversion of wavelength to wave number has to be made a $1/\lambda$ dependence is introduced. The difference does not have an effect on the development of different absorption peaks in time dependent measurements, which is the main reason why the new setup was developed. In the rest of this article, for the sake of clarity the optical scanner position will be converted to wavelength instead of wave number.

The calibration, which is easy to perform, has to be made every time a small change to the alignment of the setup is made, e.g., when the sample is changed or the detector signal is optimized. This is because slight movement of the detector or of a mirror will lead to a slight change in wavelength measured at the detector at a specific angle of the optical scanner.

VI. SENSITIVITY

Various substrate types can be used as was shown in Sec. I. There it was shown that it is easiest to use the setup in two

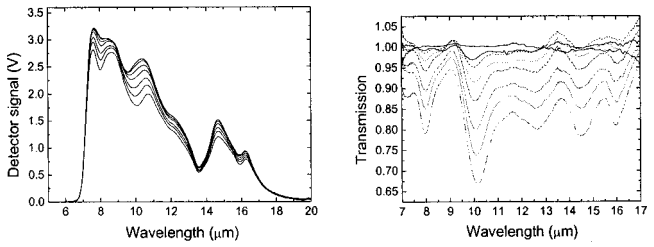

FIG. 8. Corrected detector signal and calculated reflection spectra at various times during silicon oxide like film deposition obtained in single reflection mode; time interval between measurements shown=6.6 s.

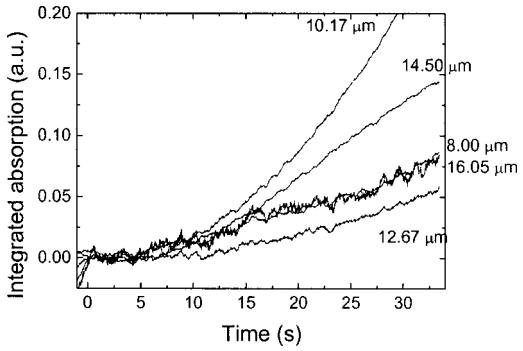

FIG. 9. Integrated absorption intensity for various absorption peaks observed during silicon oxide like film deposition as a function of time in single reflection mode.

different modes. First, the setup is used in single reflection mode and then in ATR mode. The absorption sensitivity is obviously different in these two modes.

To demonstrate the sensitivity and time resolution of the fast reflection absorption setup an expanding thermal plasma deposition setup is used. This deposition setup has been depicted in the literature extensively and therefore only a short description of the setup will suffice.[25,26] A thermal argon plasma is generated by a cascaded arc and expands into a vacuum vessel with a typical pressure of 10–30 Pa. Into this expanding argon plasma deposition precursor gases are injected by a punctured injection ring situated 5 cm from the arc exit or by an injection nozzle.[13] The precursor injected will be dissociated by interaction with the argon plasma. The dissociated species will cause film deposition to occur at the substrate which is situated on top of a chuck with a thermostrat 65 cm from the arc exit. The deposition is monitored by the fast infrared reflection absorption spectroscopy setup and the film thickness is monitored by *in situ* ellipsometry. For the demonstration HMDSO and oxygen are used as film deposition precursors.

VII. SINGLE REFLECTION

In Fig. 8 the evolving detector signal, corrected for the background signal, as a function of the wavelength at various times during HMDSO/oxygen deposition are shown (deposition rate 10.0 nm/s). It can be seen that the maximum value of the detector signal is approximately 3.2 V which is, as expected, above the predicted 2.2 V. In Fig. 8 the reflection absorption spectra at various times during film growth are also shown. It can be seen that various absorption peaks appear and grow during the deposition process. Notice that the spectra shown are single spectra, each obtained in 2.5 ms, and that they have not been averaged. For the sake of clarity only a couple of spectra are shown.

The noise level can also be observed in Fig. 8 if the first reflection spectrum is studied in more detail. This first spectrum was obtained when there was still no deposition on top of the sample and therefore it is a good indication of the noise level. For longer wavelengths the noise present in this reflection spectrum is larger than for shorter wavelengths. This is in agreement with the measured detector signal, the higher the detector signal the lower the relative noise in the detector signal and the lower the noise in the calculated reflection spectrum. The absolute value of the noise level measured is in agreement with the expected noise level (10^{-2}). It is not possible to measure the absorption of any absorption peak, not even the strongest one, at monolayer sensitivity (2×10^{-4}).

A better way to present evolution of the absorption peak as a function of time, without skipping measured spectra, is by integrating the various absorption peaks in every individual absorption spectrum. Integration was done by fitting a baseline to every absorption peak and integrating the area between the absorption and its baseline. An example of the integrated absorption intensity as a function of time is given in Fig. 9. It can be seen that the integrated absorption has a noise level which is different for different absorption peaks. This difference in absorption is caused by the spectral detector signal, which causes noise in the calculated reflection absorption spectrum to depend on the position in the spectrum.

The scanning time and time resolution of the data shown in Figs. 8 and 9 were chosen as 2.5 ms as mentioned before. This time scale is not the fastest possible, but at this time scale the scanning angle could be higher and therefore second order diffraction of the first absorption peak (at 16.05 μm) could also be measured. This reflection absorption intensity was also integrated and is also shown in Fig. 9. It can be seen that the evolution of this peak as a function of time is similar to the evolution of this reflection absorption peak observed in first order as was expected. The integrated absolute absorption intensity is different but that is due to the fact that absorption was treated in the same way as the other absorption peaks in first order. To convert the scanner angle to wavelengths it was assumed that all data were first order and therefore the width of the second order peaks in the wavelength spectrum is different from the one measured in first order. The peak absolute absorption intensity is however the same and thus the integrated absorption intensity is different. Physical interpretation of the data shown in Figs. 8 and 9 will not be made here. Notice that *in situ* measurements of the same deposition at a faster speed would have resulted in the same signal to noise ratio for the integrated absorption intensity.

The integrated absorption intensity can be smoothed by adjacent averaging. This will show the evolution of the absorption intensity more clearly, but it will lead to loss of detail in the deposition processes which take place on a shorter time scale than the time scale represented by the av-

eraging interval. So when studying the initial growth process of a film only processes slower than the measuring time scale can be observed. For steady state film growth adjacent averaging will not influence the results. For the data shown in Fig. 9 five point adjacent averaging was used.

Notice that the conditions used, the fast *in situ* infrared reflection absorption spectroscope will not detect the HMDSO gas phase absorption during deposition. This is because during deposition the absolute density of HMDSO in the gas phase is too low to be detected. During deposition the pressure in the plasma reactor is 10 Pa and less than 5% of the gas is the deposition precursor gas. During a deposition experiment the precursor is injected into the plasma and a large amount (approximately 70%) of it is consumed by the plasma. So less than 1.5% of 10 Pa is HMDSO gas and thus the HMDSO partial pressure is less than 0.15 Pa, which is only 1/333 of the pressure used for gas phase calibration measurements (cf. Fig. 7). Therefore the absorption intensity of the strongest absorber of this small amount of HMDSO ($0.25/333=7.5\times10^{-4}$) will be below the sensitivity of the spectroscope (10^{-2}). Notice that the gas phase absorption intensity is of the same order as the monolayer absorption intensity. By increasing the sensitivity it is therefore possible that the contribution due to the gas phase cannot be neglected and a correction needs to be made. Eliminating the gas phase contribution can be done by using a polarizer and performing the experiment twice at different polarization angles.

VIII. ATR

To enhance the absorption signal an ATR crystal can be used.[4,5,27,28] In the crystal light will have multiple internal reflections, and due to these the light will also have multiple interactions with the film deposited on top of the ATR crystal. In these experiments ZnSe ATR crystals were chosen. ZnSe has good transparency in the infrared and also reasonable transparency in the visible, which makes the aligning procedure of the setup easier because the path of light can be observed without using any infrared light detecting device.

The refractive index of ZnSe in the range of 5–10 μm is approximately equal to 2.4. The refractive index of the deposited silicon oxide film is about 1.4 and the angle of light, with respect to the ATR crystal surface, in the ATR crystal is approximately 55°. This is above the critical angle[4] for total internal reflection which is approximately 35° and therefore light will not propagate into the film deposited on top of the crystal. Absorption will occur in the evanescent wave that occurs at the surface on which total internal reflection takes place.[4] Light will pass through the film twice, once upon entering the crystal and once upon leaving the crystal. This will also cause transmission absorption, which is different from reflection absorption. However, this will only be a small fraction of the total absorption, e.g., with 35 reflections this fraction will be 2/37.

In Fig. 10 infrared reflection absorption spectra obtained using an ATR crystal are shown for HMDSO/oxygen deposition similar to that shown for single reflection mode. Again, only selected spectra are shown for the sake of clarity and no

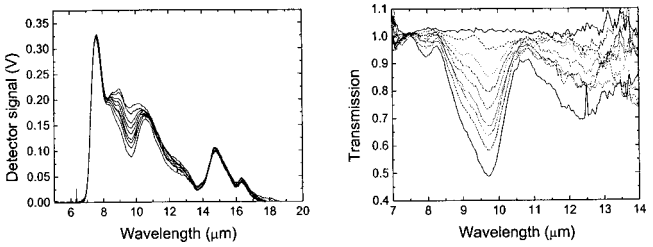

FIG. 10. Measured detector signal and calculated reflection spectra at various times during silicon oxide like film deposition obtained in ATR mode; time interval between measurements shown=0.45 s.

spectra averaging was done. The infrared absorptions are more intense than in the case of single reflection. In Fig. 10 the corrected detector signal as a function of the wavelength is also shown. A comparison of the maximum detector signal with the maximum signal obtained in single reflection mode (see Fig. 8) shows that the signal decreased one order of magnitude, where as a reduction with a factor of 5 was expected. This difference is probably due to the alignment of the setup, which is more critical in the case of ATR mode than in single reflection mode. This is due to the focusing on the initial bevel of the ATR crystal.

A comparison of the reflection absorption spectra obtained in ATR mode with the reflection absorption spectra obtained in single reflection mode shows some differences. Notice that in the case of ATR mode a smaller part of the spectrum is plotted due to which two reflection absorption peaks are not plotted. In the part omitted the noise level is too high to get a clear picture, and this was already be observed on the higher wavelength side of the reflection absorption spectrum shown in Fig. 10. The first difference is that the peak at 8 μm is much smaller with respect to the peak with biggest reflection absorption intensity in ATR mode than in single reflection mode. The second difference that can be seen is that the shape of the various absorption peaks is different and that the position of the maximum reflection absorption intensity is slightly shifted. Both differences are due to the change of substrate material when changing from single reflection mode to ATR mode.

A similar difference is observed between a reflection absorption spectrum and the transmission absorption spectrum on the same substrate material.[4] Due to absorption the imaginary part of the refractive index as a function of the wavelength is not equal to zero at the wavelength of absorption. Therefore the Fresnel coefficients for reflection as a function of the wavelength will change locally which results in a change in reflection. The Fresnel coefficients also depend on the refractive index of the substrate material and because the film deposited on top of the silicon substrate is similar to the film deposited on top of the ZnSe ATR crystal the change in the reflection absorption spectrum can only be due to the difference in substrate material. A calculation using the Fresnel equations fully supports this theory.[29]

To get better insight into the development of the various absorption peaks, the absorption peaks are integrated and plotted as a function of time. The result is shown in Fig. 11. Five point adjacent averaging was used to smooth the integrated absorption data. The data in Fig. 11 indicate that the

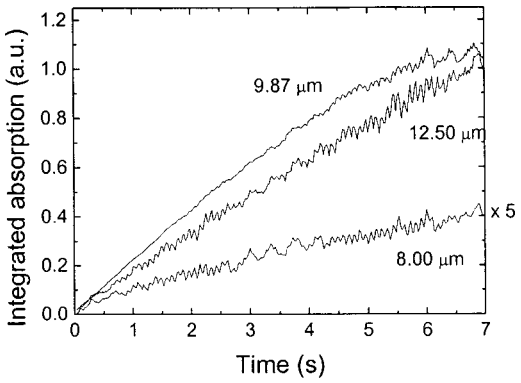

FIG. 11. Integrated absorption intensity for various absorption peaks observed during silicon oxide like film deposition as a function of time in ATR mode.

absorption intensity is much stronger than in the case of single reflection (cf. Fig. 9). However, it is not possible to give an exact value for the increase in absorption intensity because the substrate material for the two modes is different. An increase of a factor of 35 was expected, and looking at the strongest absorption peak it can be seen that indeed an increase close to this value is reached. However, the sensitivity of the ATR setup is not 35 times as high as in single reflection. This can be seen in the noise level of the ATR absorption spectra taken before deposition started. In these spectra the absolute noise level (4×10^{-2}) is higher than that in the single reflection absorption spectrum (1×10^{-2}). This is due to the fact that the absolute infrared intensity on the detector is decreased by installing an ATR crystal in the setup. This lower intensity will lead to a relatively higher noise level in the signal detected and therefore higher absolute noise in the ATR absorption spectra with respect to in the single reflection absorption spectra. Although the absolute noise level is higher still the absorption sensitivity is increased and therefore the absorption of thinner films can be measured *in situ* with high time resolution. Taking the absorption intensity to be 35 times that of single reflection mode than a single reflection equivalent absorption of approximately 1×10^{-3} can be measured, which is in agreement with the predictions.

The sensitivity can be increased even more by averaging multiple spectra, but it should be realized that this will result in lower time resolution. For deposition rates of only a couple of nanometers per second this does not have to be a problem, because with the deposition of one monolayer up to 100 spectra can be obtained. Averaging 100 spectra will result in an increase in sensitivity by a factor of 10. If this setup were used for analysis of silicon oxide-like film deposition it would improve the sensitivity to monolayer sensitivity. In using this setup it is best to find a balance between time scale, sensitivity, and averaging.

[1] M. Meier and A. von Keudell, J. Appl. Phys. **90**, 3585 (2001).
[2] H. Ohta, M. Hori, and T. Goto, J. Appl. Phys. **90**, 1955 (2001).
[3] P. Scheible and A. Lunk, Thin Solid Films **364**, 40 (2000).
[4] N. J. Harrick, *Internal Reflection Spectroscopy* (Wiley, New York, 1967).
[5] J. R. During, *Applications of FT-IR Spectroscopy* (Elsevier, Amsterdam, 1990).
[6] S. A. Francis and A. H. Ellison, J. Opt. Soc. Am. **49**, 131 (1959).
[7] Y. Toyoshima, K. Arai, A. Matsuda, and K. Tanaka, Appl. Phys. Lett. **56**, 1540 (1990).
[8] N. Maley, I. Szafranek, L. Mandrell, M. Katiyar, J. R. Abelson, and J. R. Thornton, J. Non-Cryst. Solids **114**, 163 (1989).
[9] J. W. A. M. Gielen, P. R. M. Kleuskens, M. C. M. van de Sanden, L. J. van Ijzendoorn, D. C. Schram, E. H. A. Dekempeneer, and J. Meneve, J. Appl. Phys. **80**, 5986 (1996).
[10] W. M. M. Kessels, A. H. M. Smets, B. A. Korevaar, G. J. Adriaenssens, M. C. M. van de Sanden, and D. C. Schram, Mater. Res. Soc. Symp. Proc. **557**, 25 (1999).
[11] A. de Graaf, G. Dinescu, J. L. Longueville, M. C. M. van de Sanden, D. C. Schram, E. H. A. Dekempeneer, and L. J. van Ijzendoorn, Thin Solid Films **333**, 29 (1998).
[12] J. W. A. M. Gielen, M. C. M. van de Sanden, P. R. M. Kleuskens, and D. C. Schram, Plasma Sources Sci. Technol. **5**, 492 (1996).
[13] M. F. A. M. van Hest, B. Mitu, D. C. Schram, and M. C. M. van de Sanden (unpublished).
[14] R. Raghavan and P. W. Morrison, Jr., J. Quant. Spectrosc. Radiat. Transf. **69**, 605 (2001).
[15] A. T. M. Wilbers, G. M. W. Kroesen, C. J. Timmermans, and D. C. Schram, Meas. Sci. Technol. **1**, 1326 (1990).
[16] A. T. M. Wilbers, G. M. W. Kroesen, C. J. Timmermans, and D. C. Schram, J. Quant. Spectrosc. Radiat. Transf. **45**, 1 (1991).
[17] J. T. Houghton and S. D. Smith, *Infrared Physics* (Oxford University Press, Oxford, 1966).
[18] F. L. Pedrotti and L. S. Pedrotti, *Introduction to Optics* (Prentice–Hall, Englewood Cliffs, NJ, 1993).
[19] C. Palmer, Diffraction Grating Handbook, Richardson Grating Laboratory, Rochester NY (2000).
[20] S. P. Davis, *Diffraction Grating Spectrographs* (Holt, Rinehart, and Winston, New York, 1970).
[21] *Spectrometric Techniques IV*, edited by G. A. Vanasse (Academic, New York, 1985).
[22] M. M. Hemerik, Ph.D. thesis, Eindhoven University of Technology, Eindhoven, The Netherlands, 2001.
[23] Y. Segui and P. Raynaud, NATO ASI Ser., Ser. C **346**, 81 (1997).
[24] M. C. Hutley, *Diffraction Gratings* (Academic, London, 1982).
[25] J. W. A. M. Gielen, W. M. M. Kessels, M. C. M. van de Sanden, and D. C. Schram, J. Appl. Phys. **82**, 2643 (1997).
[26] A. de Graaf, Ph.D. thesis, Eindhoven University of Technology, Eindhoven, The Netherlands, 2000.
[27] N. J. Harrick, Phys. Rev. Lett. **4**, 224 (1960).
[28] E. S. Aydil, R. A. Gottscho, and Y. J. Chabal, Pure Appl. Chem. **66**, 1381 (1994).
[29] M. F. A. M. van Hest, Ph.D. thesis, Eindhoven University of Technology, Eindhoven, The Netherlands, 2002.
[30] H. G. Pryce Lewis, T. B. Casserly, and K. K. Gleason, J. Electrochem. Soc. **148**, F212 (2001).
[31] D. Magni, Ch. Deschenaux, Ch. Hollenstein, A. Creatore, and P. Fayet, J. Phys. D **34**, 87 (2001).